A New Height-Estimation Method Using FMCW Radar Doppler Beam Sharpening

Amir Laribi,
Markus Hahn
and Jürgen Dickmann
Daimler AG, Research Center Ulm
Environment Perception
Ulm Germany
Email: amir.laribi@daimler.com

Christian Waldschmidt
Ulm University
Intitute of Microwave Techniques, Ulm
Email: christian.waldschmidt@uni-ulm.de

Abstract—This paper presents a new method for estimating the height of extended objects using a Frequency Modulation Continuous Wave (FMCW) automotive radar. The proposed algorithm exploits the frequency shift caused by the Doppler effect while approaching stationary objects, to estimate target heights. Thus, the algorithm does not require multiple vertical antennas for height finding. First, the measured radial velocity is derived using sensor target geometry, then, a target height is formulated as a function of target range, vehicle velocity and elevation angle component of the measured radial velocity. Next, the processing pipeline of the proposed Doppler Beam Sharpening (DBS) algorithm is described, and the three dimensional (3D) high resolution RELAX is applied to collected radar data to provide accurate range, azimuth angle and Doppler estimations of the detected targets. Finally height measurement results of an entrance gate $4.5\ m$ high are presented and discussed. The results show that the proposed height finding algorithm can achieve a root mean squared error of $0.26\ m$.

I. Introduction

The task of resolving the height of extended objects in a vehicle's surroundings plays a major role in active safety, notably when it comes to autonomous driving. Consider a situation in which based on received radar data, the collision avoidance system of an autonomous driving car has to decide whether a detected target represents an imminent collision or merely a traversable bridge. Another example are parking scenarios where the autonomous vehicle has to drive over a lowered curb and park, and therefore the curb's height needs to be classified as traversable. The same challenge applies while driving into a garage where the driving pilot has to determine whether the received object's echoes are coming from an obstacle, or if they are simply edge reflections due to some parts of the door's frame.

Many approaches in different fields [1] [2] have been recently proposed to estimate target heights. For automotive applications, a bridge identification algorithm [3] based on a multipath interference pattern was proposed. The applied pattern consisted of variation in the back-scattered power from the phase differences of the direct path to the target and the indirect path, while driving towards bridges or stationary obstacles. In the previous work [4] [5], results of height measurement trials conducted on extended targets located at

short ranges (less than $7\ m$) proved that the height of point targets can be accurately estimated by exploiting the range difference information between line-of-sight (LOS) and non-line-of-sight (NLOS) components of radar waves. In this paper, height determination of targets located at mid- and long-ranges is investigated, in particular, the height estimation of bridges and entrance gates.

The remainder of this work is organized as follows: Section II formulates a target height based on the measured radial velocity and sensor target geometry. Section III discusses the different scattering mechanisms of radar waves, focusing on the knife-edge effect. Section IV describes the 3D processing pipeline of the DBS height-finding algorithm. Section IV provides the results of the proposed algorithm. Section VI contains the conclusion.

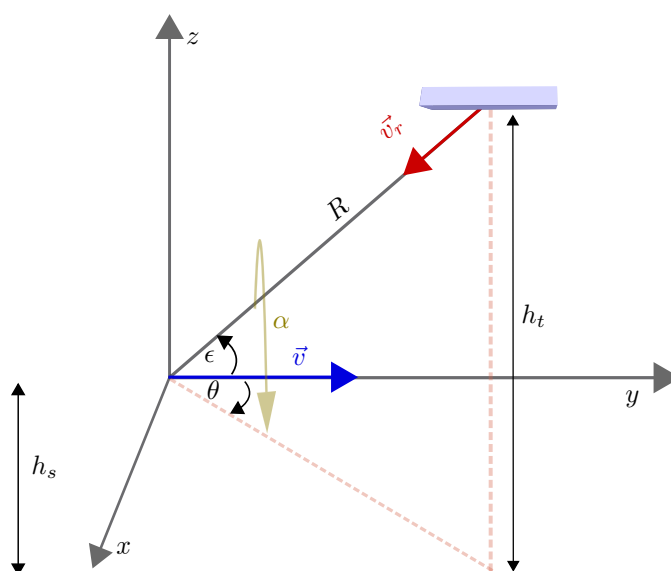## II. Doppler Beam Sharpening Geometry Model

Fig. 1. Geometry for target height formulation using Doppler Beam Sharpening.

This section describes the geometry model for target height estimation using Doppler information. Assuming a vehicle driving towards a stationary object at a velocity v, a radar sensor mounted at the front of the vehicle will measure a radial velocity v_r of the observed target which is given by.

$$v_r = -v \cos(\alpha), \qquad (1)$$

where v_r is the length of a vector $\vec{v_r}$ in a spherical coordinate system pointing towards the sensor at an angle α between the velocity vector of the vehicle and the line of sight to target. The angle α includes both a horizontal (azimuth) and a vertical (elevation) angle component θ and ϵ, so that (1) can be written as follows

$$v_r = -v \cos(\theta) \cos(\epsilon). \qquad (2)$$

Hence the radial velocity component $v_{r_{el}}$ that is dependent on the elevation angle ϵ can be formulated as

$$v_{r_{el}} = -v \cos(\epsilon) = \frac{v_r}{\cos(\theta)}. \qquad (3)$$

Using geometry the target height h_t is given by

$$h_t = h_s + R \sin(\epsilon), \qquad (4)$$

where R and h_s denote the range from radar sensor to target and the sensor height respectively. Using (3), h_t can be written as a function of v, v_{el}, R and h_s

$$h_t = h_s + R \sin(\arccos(-\frac{v_{r_{el}}}{v})). \qquad (5)$$

III. Scattering Mechanisms and the Diffraction Phenomenon

In this section, the three main scattering mechanisms, i.e, reflection, diffraction, and refraction of radar waves in the order of their contribution to the radar cross section (RCS) are briefly discussed and the Knife-edge diffraction phenomenon is presented, the knife-edge effect makes it possible to assume that the ground truth height of the gate entrance is measured at the gate's lower edge. When electromagnetic waves impinge on an object, the received scattered field of the object at the antenna corresponds to the sum of radiations reaching the receiver from different target parts (features). Depending on the features' geometry, target material property, target size and the emitted wave length, the radiation of energy can be dictated by various scattering mechanisms. If the Poynting vector [6] of the incoming wave is perpendicular to a flat part of the target, the most dominant contribution to the scattered target energy at the receiver will be a specular echo. Specular reflections follow the law of reflections, the incident and the outgoing wave form the same angle with respect to the normal of the surface. As the angle of incidence moves away from the surface normal, specular echoes are redirected away from the receiving antenna and the second largest contribution to the scattered field is due to diffraction. Diffraction occurs when there are discontinuities in the target geometry such as edges, wedges, corners and tips or when there is a discontinuity in the electromagnetic material properties of the target features.

Echoes induced by edges and wedges are particularly strong. This kind of scattering is known as knife-edge diffraction or the knife-edge effect. If the curvature radius of the edge is at least a wavelength or two, the echo is larger for any incident polarization. Otherwise, the echo is stronger when the incident electric field is parallel to the edge [6]. Another scattering mechanism is refraction or bending, this phenomenon occurs in free space when radar waves reach the atmosphere.

In this work, the most important contribution of the radiated energy from target to sensor, is assumed to be due to diffraction mechanisms. This type of scattering, in particular the knife-edge effect, ensures the scattered energy will be radiated mainly from edges of targets such as bridges and gates.

IV. Algorithm Overview

In this section, the processing steps of the proposed DBS height finding algorithm are presented. First, a coarse 3D Fast Fourier Transform (FFT) is applied to the received beat signals, to provide an initial range, azimuth angle and Doppler estimates. Subsequently, target detection is performed and the number of detected targets is computed. Finally a high resolution range, azimuth angle and Doppler spectrum is calculated using the 3D RELAX [7] algorithm and the heights of the extracted targets are estimated using the DBS geometry model in (5).

A. 3D-FFT Range Angle and Doppler Processing

The received beat signal contains information about the target range, Doppler and the direction of arrival (DOA), the DOA information is obtained from L azimuth antennas of a Multiple Input Multiple Output (MIMO) radar. Hence, the received signal can be expressed as

$$s_{IF}(n, l, m) = a \, e^{j2\pi f_b n} e^{j2\pi \frac{d \sin(\theta) l}{\lambda}} e^{j2\pi f_d T m}, \qquad (6)$$

where a is the signal amplitude, f_b is the range beat frequency, f_d is the Doppler-frequency, λ is the wave length, θ is the target azimuth angle of arrival, T is the chirp duration time, d is the spacing between the antenna elements. $n = 0, 1, ..., N - 1$, $l = 0, 1, ..., L - 1$ and $m = 0, 1, ..., M - 1$, where L, N and M denote the number of received channels, the number of samples per chirp and the number of ramps per frame respectively. To extract the range beat frequency term, a Hanning window function $w(n)$ is first applied the 3D cube along the fast time dimension to reduce side-lobes. The windowed signal is then taken to the frequency domain by applying an FFT along the same dimension, The Range FFT is performed using $2K_r$ FFT points, and is given by

$$X(k_r, l, m) = \sum_{n=0}^{N-1} s_{IF}(n, l, m) \, w(n) \, e^{-\frac{j2\pi n k_r}{N}}, \qquad (7)$$

with $k_r = 0, 1, ..., 2K_r - 1$, where K_r is the number of range bins. After the range FFT, the symmetrical half of the spectrum corresponding to negative frequencies is removed, thus the number of bins is divided by two, leading to K_r range bins.

The second step in (8) consists of retrieving the target angle term. This can be achieved using digital beam forming technique (DBF) [8], multiplying the data from (7) with a window function $w(l)$ and applying a second FFT. The windowing and the FFT are applied this time along the antenna elements

$$X(k_r, k_\theta, m) = \sum_{l=0}^{L-1} X(k_r, l, m)\, w(l)\, e^{-\frac{j2\pi l k_\theta}{L}}, \qquad (8)$$

with $k_\theta = 0, 1, ..., K_\theta - 1$, where K_θ is the number of angle bins.

Finally, a third FFT is applied along the slow time dimension to compute the Doppler information for each frame. The Hanning window function $w(l)$ is applied to the data cube obtained from (8). This is given by (9)

$$X(k_r, k_\theta, k_d) = \sum_{m=0}^{M-1} X(k_r, k_\theta, m)\, w(m)\, e^{-\frac{j2\pi m k_d}{M}}, \qquad (9)$$

with and $k_d = 0, 1, ..., K_d - 1$, where K_d denotes the number of Doppler bins.

B. Target Detection

After the 3D processing of the received beat signal, a Doppler bin magnitude maximum search is performed over the power spectral density (PSD). This means that the bin search is carried out along the Doppler bin dimension of the 3D spectrum cube obtained from (9), for each range and angle bin pair (k_r, k_θ). The resulting two dimensional (2D) matrix is $X(k_r, k_\theta, k_{d_{max}})$, where

$$k_{d_{max}} \in \max |X(k_d)|\, \forall (k_r, k_\theta), \qquad (10)$$

is a fixed Doppler bin. Next, a 2D cell average-constant false alarm rate (CA-CFAR) [9] is applied to the 2D spectrum matrix in range and angle, to discriminate target peaks from clutter. This is done by calculating an adaptive threshold of the 2D Peaks, using a sliding window which is centered at every (k_r, k_θ) cell in the 2D matrix. The threshold is then computed by averaging and scaling the neighboring PSD cells of the center cell. After the target discrimination, dense detections output by the CA-CFAR algorithm are merged into clusters by the Density-based spatial clustering of applications with noise algorithm (DBSCAN) to yield K targets.

C. High Resolution 3D Spectral Estimation Using RELAX

To achieve accurate height estimations using Doppler Beam Sharpening, the target 3D parameters have to be estimated as accurately as possible. In this work, a 3D RELAX was implemented to allow for high resolution range, angle and Doppler estimation. After target extraction, a high resolution 3D PSD is obtained from the beat signal in (6) using 3D RELAX. RELAX [7] is a parametric high resolution algorithm which relies on a nonlinear regression model to estimate the frequencies present in a signal as well as their respective amplitudes. To estimate the 3D parameter of the

extracted K targets, RELAX assumes that received radar signal $S_{IF}(n, l, m)$ in (6) can be modeled as the sum of multiple weighted complex exponentials plus noise, so that $S_{IF}(n, l, m)$ can be described by the following model

$$y_{n,l,m} = \sum_{k=1}^{K} a_k\, e^{j2\pi f_k n} e^{j2\pi f'_k l} e^{j2\pi f''_k m} + e_{n,l,m}. \qquad (11)$$

Where $n = 0, 1, ..., N - 1$, $l = 0, 1, ..., L - 1$ and $m = 0, 1, ..., M - 1$. L, N and M denote the number of received channels, the number of samples per chirp and the number of ramps per frame respectively. The variable a_k denotes the unknown complex amplitude, and f_k, f'_k and f''_k are the unknown range, angle and Doppler frequencies of the k-th harmonic respectively. for $k = 1, 2, ..., K$; $e_{n,l,m}$ denotes the noise. The sinusoidal parameters $\{\hat{f}_k, \hat{f}'_k, \hat{f}''_k, \hat{a}_k\}$ can be obtained by recursively minimizing the following nonlinear least-squares cost function

$$C_l(\{f_i, f'_i, f''_i, a_i\})_{i=0}^{K} = \| y - \sum_{k=1}^{K} a_k W(f_k) \|^2, \qquad (12)$$

where $\|.\|$ denotes the Euclidean norm, y is the N x L x M 3D beat signal cube in (6), and $W(f_k) = [W_{n,l,m}]$ is a rank 3 tensor, such that

$$W_{n,l,m} = w_n(f_k).\, w_l(f'_k).\, w_m(f''_k), \qquad (13)$$

where $w(f_k)$, $w(f'_k)$ and $w(f''_k)$ are given by

$$w(f_k) = [1\ e^{j2\pi f_k} \ ... \ e^{j2\pi f_k(N-1)}]^T,$$
$$w(f'_k) = [1\ e^{j2\pi f'_k} \ ... \ e^{j2\pi f'_k(L-1)}]^T, \qquad (14)$$
$$w(f''_k) = [1\ e^{j2\pi f''_k} \ ... \ e^{j2\pi f''_k(M-1)}]^T.$$

Let y_k be given by

$$y_k = y - \sum_{i=1, i \neq k}^{K} \hat{a}_i\, W(\hat{f}_i), \qquad (15)$$

where $\{\hat{f}_i, \hat{a}_i\}_{i=1, i \neq k}^{K}$ are assumed to be given then, minimizing the cost function in equation (12) with respect to f_k and a_k gives

$$(\hat{f}_k, \hat{f}'_k, \hat{f}''_k) = \max_{f_k, f'_k, f''_k} |< W^*(f_k), y_k >|^2, \qquad (16)$$

and

$$\hat{a}_k = \frac{1}{NLM} < W^*(f_k), y_k >, \qquad (17)$$

where $< ., . >$ denotes the sum over all element-wise products. The estimate of $(\hat{f}_k, \hat{f}'_k, \hat{f}''_k)$ can be obtained as the location of the dominant peak of the periodogram, which can be efficiently computed by the 3D-FFT of the data cube y_k, using zero padding. Finally the range $R = \frac{f_k f_s c T}{2B}$, the DOA angle $\theta = \arcsin(\frac{f'_k \lambda}{d})$ and the Doppler velocity $v_r = f''_k \frac{c}{2 f_c T}$, are extracted from $(\hat{f}_k, \hat{f}'_k, \hat{f}''_k)$. Where c denotes the speed of light, f_s denotes the sampling frequency, and B denotes the radar bandwidth. The output of the 3D Relax is shown in Fig.3
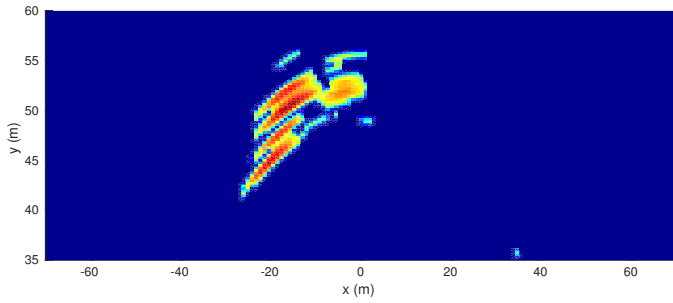
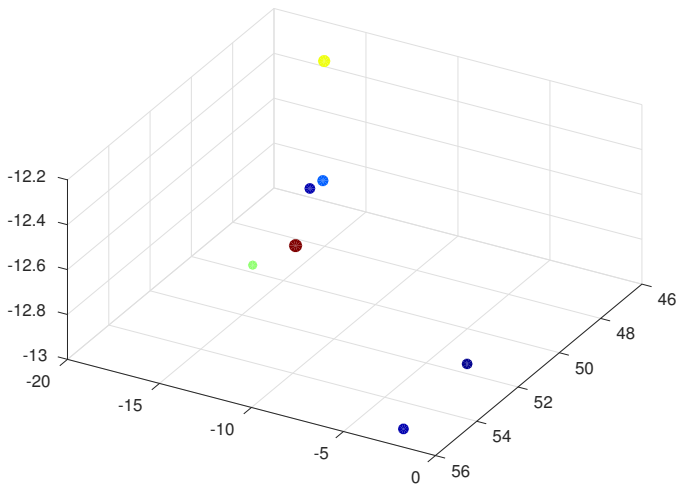Fig. 2. Cartesian Map computed using 3D-FFT.

Fig. 3. 3D-Relax output showing the same Cartesian map in Fig. 2, the Z-axis corresponds to the radial velocity of each target in the Cartesian map.

D. Target Height Estimation Using Doppler Beam Sharpening

Based on the vehicle velocity, the target range, azimuth angle and Doppler information obtained from the RELAX high resolution 3D PSD, the entrance gate height can be estimated. For each target, the computed azimuth DOA angle θ and radial velocity v_r are used to obtain the radial velocity component $v_{r_{el}}$, which is dependent on the target elevation angle ϵ. This is achieved based on (3). Next, the target height is calculated from (5) using $v_{r_{el}}$, v, R and h_s.

V. EXPERIMENTAL RESULTS

This section describes the radar measurement setup, then summarizes and discusses the height estimation results of the DBS height finding algorithm.

Fig. 4. A block diagram showing the processing steps of the Doppler beam sharpening height-finder algorithm.

A. Measurement Setup

In the following experiment, a 77 GHz mid-range MIMO radar with 300 MHz bandwidth was used, the radar is a time division multiplexed (TDM) system with two transmitting (Tx) co-located antennas and 10 receiving (Rx) antennas. The Tx antennas are each capable of sending 128 fast ramps per cycle, the radar sensor was mounted on the front of the car $0.5\ m$ above the ground. The vehicle drove towards a facility entrance at a velocity varying between $11.11\ m/s$ and $13.33\ m/s$. The entrance gate, which was illuminated by the radar sensor, has an upper edge height of $5\ m$ and a lower edge height of $4.5\ m$. For each measurement cycle, 256 target echoes, the vehicle velocity, and the corresponding echo and velocity time stamps were recorded. The velocity of the car was provided by an Automotive Dynamic Motion Analyzer (ADMA) device in the vehicle. Hence, the received data for each measurement cycle consisted of 10 x 512 x 256 samples, where the first dimension is the number of channels, the second dimension is the number of time samples per channel, and the third dimension is the number of chirps per channel. To achieve a higher accuracy and resolution of azimuth DOA estimation, a larger virtual aperture is constructed from the original cube to yield a 3D cube containing 19 x 512 x 128 data samples. The height of the entrance gate was estimated by processing the received 3D data cube and the corresponding vehicle velocity data at each cycle.

Fig. 5. The entrance gate of the facility (target). The gate is $16.5\ m$ wide and $4.5\ m$ high (lower edge height). The radar sensor was mounted at $0.5\ m$ above the ground on the front of the vehicle. The car drove at a velocity between $11, 11\ m/s$ and $13.33\ m/s$ towards the gate while echoes of the target were simultaneously being recorded.

B. Results

Fig. 6 summarizes the height results, estimated by the proposed Doppler beam sharpening algorithm. During the measurement campaign, the vehicle drove toward the entrance gate three times. Hence, three datasets were collected and processed by the height finding algorithm. After processing, target heights measured at the same range cell were averaged. the cell size was set to $1\ m$ To suppress detections of

targets other than the gate entrance, two field of view (FOV) thresholds were set depending on the target measured range and the sensor azimuth and elevation field of view. Thus, heights of objects out of the FOV were not considered. As illustrated in Fig. 4, the proposed algorithm can measure the gate height with high accuracy. In the first dataset (blue color), a root mean square error (RMSE) of $0.8\ m$ was measured. The largest mean error measured was $1.14\ m$ at $61.5\ m$ range. At $48.5\ m$ range, the RMSE was $0.95\ m$. In the second dataset (orange color), the RMSE was $0.63m$, with a largest mean error of $1.08\ m$ below ground truth at $54.5\ m$ range. An RMSE of $0.26\ m$ was calculated for the third dataset (yellow color), with a largest measured deviation of $0.82\ m$ at $49.5\ m$ range. Fig. 6 shows also a discrepancy at some range bins between measured height results of the third dataset and the results of both the first and the second dataset. This difference could be related to many factors such as engine induced car-body vibrations, vehicle acceleration, steep grounds or the coherency of the received ramps. The impact of these factors on the accuracy of the DBS height-estimation algorithm will be investigated in future work.
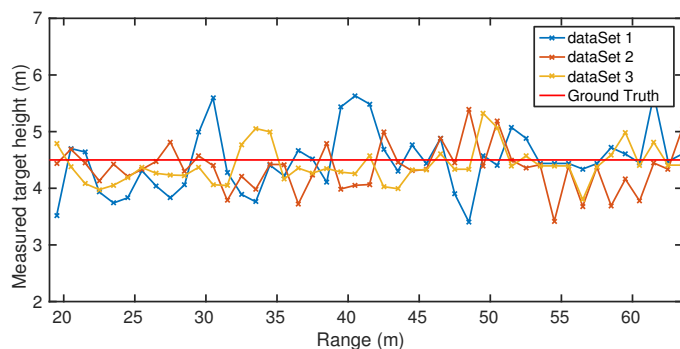

Fig. 6. Measured target height outputs of the proposed DBS algorithm. The figure shows three curve extensions of three datasets (blue, orange, yellow), corresponding to three runs towards the entrance gate. starting at a maximum range of $64\ m$ and stopping at a range of $19\ m$

VI. Conclusion

In this work, a Doppler-based height finder algorithm using a 77 GHz mid range FMCW radar was proposed. Radar echoes of a $4.5\ m$ high gate were recorded during different driving trials, processed, and the corresponding height measurement results were presented and discussed. It can be concluded that height estimation of extended targets can be resolved with high accuracy by exploiting the frequency shift of radar waves, caused by the Doppler effect, while approaching targets. The presented height results show that the proposed algorithm can determine whether a detected target is traversable or not.

References

[1] J. Habonneau, J.-M. Le Caillec, A. Khenchaf, and L. Mandridake, "Multipath height estimation of target reflectors," in *2013 14th International Radar Symposium (IRS)*, vol. 1. IEEE, 2013, pp. 258–263.

[2] P. Phu, H. Aumann, and J. E. Piou, "Multipath height finding in the presence of interference," in *2007 IEEE Antennas and Propagation Society International Symposium*, 2007.

[3] F. Diewald, J. Klappstein, F. Sarholz, J. Dickmann, and K. Dietmayer, "Radar-interference-based bridge identification for collision avoidance systems," in *Intelligent Vehicles Symposium (IV), 2011 IEEE*. IEEE, 2011, pp. 113–118.

[4] A. Laribi, M. Hahn, J. Dickmann, and C. Waldschmidt, "A novel target height estimation approach using radar wave multipath propagation for automotive applications," in *Kleinheubacher Tagung, MS No.: ars-2016-47, IRS 2016*. ARS, 2016.

[5] ——, "Vertical digital beamforming versus multipath height finding," in *International Conference on Microwaves for Intelligent Mobility, ICMIM 2017*. IEEE, 2017.

[6] M. T. T. Eugene Knott, John F. Schaeffer, *Radar Cross Section*. Scitech Publishing Inc; Auflage: 2 Rev ed. l,ISBN-10: 1891121251, 2004, vol. 2.

[7] J. Li and P. Stoica, "Efficient mixed-spectrum estimation with applications to target feature extraction," *Signal Processing, IEEE Transactions on*, vol. 44, no. 2, pp. 281–295, 1996.

[8] P. Barton, "Digital beam forming for radar," *Communications, Radar and Signal Processing, IEE Proceedings F*, vol. 127, no. 4, pp. 266–277, 1980.

[9] H. Rohling, "Radar cfar thresholding in clutter and multiple target situations," vol. AES-19,. IEEE, 1983, pp. 608–621.